

SUPPORTING INFORMATION

Synthesis, Structure and Magnetic behavior of iron arsenites with hierarchical magnetic units

Leclercq Bastien^a, Houria Kabbour^a, Angel M. Arevalo-Lopez^a, Sylvie Daviero-Minaud^a, Claire Minaud^b, Rénald David^a and Olivier Mentré^{a,*}

^a UCCS, UMR-CNRS 8181, Bâtiment C7 Ecole Centrale, Université Lille, Avenue Mendeleiev, 59655 Villeneuve d'Ascq, France.

^b Institut Chevreul, Bâtiment C4, Université Lille, Cité scientifique, 59655 Villeneuve d'Ascq, France.

* : corresponding author

Table of contents

S1. Synthesis strategies Aspects.....	S4
<i>Figure S1. Superposition of the Pourbaix diagrams of Iron and Arsenic species.....</i>	<i>S4</i>
S2. Structural and refinement datas.....	S5
<i>Table S2a. Atomic positions and equivalent isotropic thermal displacement for Ba₂Fe(As₃O₆)₂.H₂O</i>	<i>S5</i>
<i>Table S2b. Anisotropic thermal displacement for Ba₂Fe(As₃O₆)₂.H₂O</i>	<i>S5</i>
<i>Table S2c. Pertinent interatomic distances (Å) and corresponding bond-valence sum calculations for Ba₂Fe(As₃O₆)₂.H₂O</i>	<i>S6</i>
<i>Table S2d. Atomic positions and equivalent isotropic thermal displacement for BaFe₂As₂O₅AsO₃OH.....</i>	<i>S7</i>
<i>Table S2e. Anisotropic thermal displacement for BaFe₂As₂O₅AsO₃OH.....</i>	<i>S7</i>
<i>Table S2f. Pertinent interatomic distances (Å) and corresponding bond-valence sum calculations for BaFe₂As₂O₅AsO₃OH.....</i>	<i>S8</i>
<i>Table S2g. Atomic positions and equivalent isotropic thermal displacement for Ba₂Fe₂O(As₂O₅)₂.....</i>	<i>S8</i>
<i>Table S2h. Anisotropic thermal displacement for Ba₂Fe₂O(As₂O₅).....</i>	<i>S8</i>
<i>Table S2i. Pertinent interatomic distances (Å) and corresponding bond-valence sum calculations for Ba₂Fe₂O(As₂O₅).....</i>	<i>S9</i>
<i>Table S2j. Atomic positions and equivalent isotropic thermal displacement for Fe₃(As₂O₅)(AsO₃)Cl.....</i>	<i>S9</i>
<i>Table S2k. Anisotropic thermal displacement for Fe₃(As₂O₅)(AsO₃)Cl.....</i>	<i>S10</i>
<i>Table S2l. Pertinent interatomic distances (Å) and corresponding bond-valence sum calculations for Fe₃(As₂O₅)(AsO₃)Cl.....</i>	<i>S10</i>
<i>Figure S2m. Representation of the lone pair (in yellow) obtained from electron localisation function (ELF) calculations.....</i>	<i>S11</i>
<i>Figure S2n. Infrared spectra for BaFe₂As₂O₅AsO₃OH and Fe₃(As₂O₅)(AsO₃)Cl.....</i>	<i>S12</i>
S3. EDS-SEM analysis.....	S13
<i>Figure S3. EDS-SEM analysis, and resulting formula obtained from several averaged % Atomic points acquisition.....</i>	<i>S13</i>
S4. DFT calculations details.....	S14
<i>Table S4a. Relative energies for the different magnetic configurations used to extract the magnetic exchanges parameters within Ba₂Fe(As₃O₆)₂.H₂O structure, at Ueff = 6 eV.....</i>	<i>S14</i>
<i>Figure S4b. Representation of the four ordered spin stated employed to extract the two spin exchange parameters for Ba₂Fe(As₃O₆)₂.H₂O structure.....</i>	<i>S14</i>
<i>Table S4c. Values of the geometrical parameters (distances in Å and angles in °) along the magnetic exchanges paths for BaFe₂As₂O₅AsO₃OH structure.....</i>	<i>S15</i>
<i>Table S4d. Relative energies for the different magnetic configurations used to extract the magnetic exchanges parameters for BaFe₂As₂O₅AsO₃OH.....</i>	<i>S16</i>
<i>Figure S4e. Representation of the nine ordered spin stated employed to extract the five spin exchanges parameters (J1, J2, Jd, J3, J4) for BaFe₂As₂O₅AsO₃OH structure.....</i>	<i>S17</i>
<i>Table S4f. Values of the geometrical parameters (distances in Å and angles in °) along the magnetic exchanges paths for Ba₂Fe₂O(As₂O₅)₂ structure.....</i>	<i>S18</i>
<i>Table S4g. Relative energies for the different magnetic configurations used to extract the magnetic exchanges parameters for Ba₂Fe₂O(As₂O₅)₂ structure.....</i>	<i>S18</i>
<i>Figure S4h. Representation of the five ordered spin stated employed to extract the three spin exchanges parameters for Ba₂Fe₂O(As₂O₅)₂ structure.....</i>	<i>S19</i>

<i>Table S4i.</i> Values of the geometrical parameters (distances in Å and angles in °) along the magnetic exchanges paths for $Fe_3(As_2O_5)(AsO_3)Cl$ structure.....	S20
<i>Table S4j.</i> Relative energies for the different magnetic configurations used to extract the magnetic exchanges parameters for $Fe_3(As_2O_5)(AsO_3)Cl$ structure.....	S20
<i>Figure S4k.</i> Representation of the six pertinent ordered spin stated employed to extract the global trends in couplings for $Fe_3(As_2O_5)(AsO_3)Cl$ structure.....	S21
<i>Table S4l.</i> Comparison between the crystallographically calculated BVS and obtained magnetic moment from DFT calculations for each Fe cations within the simple cell $Fe_3(As_2O_5)(AsO_3)Cl$ structure at $U = 6$ eV.....	S21
S5. Magnetic measurements details.....	S22
<i>Figure S5a.</i> Cheking purity of $Fe_3(As_2O_5)(AsO_3)Cl$ sample from powder XRD.....	S22
<i>Figure S5b.</i> $M(H)$ measurements between 0 and 9 T for $BaFe_2(As_2O_5)(AsO_3)(OH)$, $Ba_2Fe_2O(As_2O_5)_2$ and $Fe_3(As_2O_5)(AsO_3)Cl$	S22

(S1) Synthesis strategies aspect

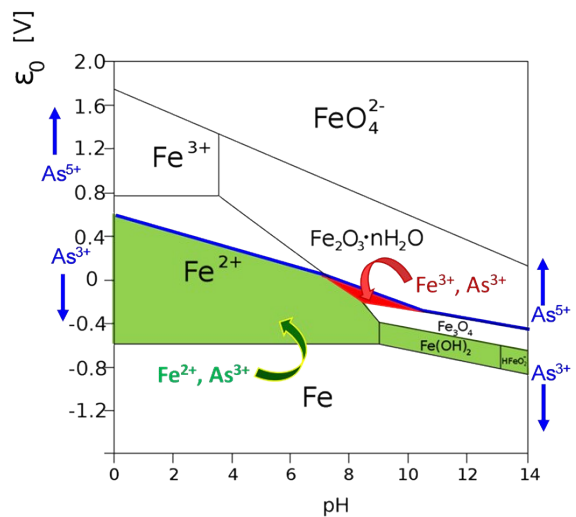


Figure S1. Schematized superposed Fe/As Pourbaix diagrams. The narrow area in red allowing the coexistence of Fe³⁺ and As³⁺ in solution (\rightarrow the formation of compound (2) and (3), prepared around pH = 9). The area in green represents the possible coexistence of Fe²⁺ and As³⁺ in solution, leading to the formation of compound (1) (prepared around pH = 7).

(S2) Structural and refinement data

Table S2a. Atomic positions and equivalent isotropic thermal displacement (in Å²) for Ba₂Fe(As₃O₆)₂.H₂O.

Atom	Wick.	Site	x	y	z	Ueq (Å²)
Ba_1	4a	1	0.4639(1)	0.5814(1)	0.0083(1)	0.0223(2)
Ba_2	4a	1	-0.4639(1)	-0.0814(1)	-0.0083(1)	0.0223(2)
As1_1	4a	1	0.3479(1)	0.3448(1)	-0.2172(2)	0.0194(4)
As1_2	4a	1	-0.3479(1)	0.1552(1)	0.2172(2)	0.0194(4)
As2_1	4a	1	0.3556 (1)	0.3243(1)	0.3154(1)	0.0191(4)
As2_2	4a	1	-0.3556(1)	0.1751(1)	-0.3154(1)	0.0191(4)
As3_1	4a	1	0.3546(1)	0.5729(1)	-0.4887(1)	0.0184(4)
As3_2	4a	1	-0.3546(1)	-0.0729(1)	0.4896(1)	0.0184(4)
Fe	4a	1	0.50000	0.25000	0.00000	0.0179(7)
O1_1	4a	1	0.4371(5)	0.6091(7)	-0.3819(12)	0.0219(19)
O1_2	4a	1	-0.4371(5)	-0.1091(7)	0.3819(12)	0.0219(19)
O2_1	4a	1	0.3954(5)	0.4653(8)	0.3472(13)	0.029(2)
O2_2	4a	1	-0.3954(5)	0.0347(8)	-0.3472(13)	0.029(2)
O3_1	4a	1	0.3130(5)	0.4778(8)	-0.3138(12)	0.0236(19)
O3_2	4a	1	-0.3130(5)	0.0222(8)	0.3138(12)	0.0236(19)
O4_1	4a	1	0.4369(6)	0.3797(9)	-0.1552(14)	0.031(2)
O4_2	4a	1	-0.4369(6)	0.1203(9)	0.1552(14)	0.031(2)
O5_1	4a	1	0.3657(7)	0.2776(10)	-0.4369(16)	0.047(3)
O5_2	4a	1	-0.3657(7)	0.2225(10)	0.4369(16)	0.047(3)
O6_1	4a	1	0.4369(5)	0.2589(9)	0.2492(14)	0.033(2)
O6_2	4a	1	-0.4369(5)	0.2411(9)	-0.2492(14)	0.033(2)
O7_1	4a	1	0.2962(4)	0.5636(15)	0.0608(12)	0.042(5)
H_1	4a	1	0.26886	0.55083	0.16736	0.042(5)
H_2	4a	1	0.26902	0.60385	-0.02384	0.042(5)

Table S2b. Anisotropic thermal displacement (in Å²) for Ba₂Fe(As₃O₆)₂.H₂O.

Atom	U₁₁	U₂₂	U₃₃	U₁₂	U₁₃	U₂₃
Ba_1	0.0410(5)	0.0115(4)	0.0143(4)	0.0014(3)	-0.0021(3)	-0.0013(3)
Ba_2	0.0410(5)	0.0115(4)	0.0143(4)	0.0014(3)	-0.0021(3)	-0.0013(3)
As1_1	0.0284(7)	0.0151(6)	0.0147(6)	-0.0025(5)	0.0023(5)	0.0023(5)
As1_2	0.0284(7)	0.0151(6)	0.0147(6)	-0.0025(5)	0.0023(5)	0.0023(5)
As2_1	0.0307(7)	0.0107(6)	0.0160(6)	-0.0003(5)	-0.0058(5)	-0.0012(5)
As2_2	0.0307(7)	0.0107(6)	0.0160(6)	-0.0003(5)	-0.0058(5)	-0.0012(5)
As3_1	0.0280(7)	0.0074(5)	0.0196(6)	0.0011(5)	0.0002(5)	0.0011(5)
As3_2	0.0280(7)	0.0074(5)	0.0196(6)	0.0011(5)	0.0002(5)	0.0011(5)
Fe	0.0278(13)	0.0081(11)	0.0179(11)	0.0014(10)	-0.0020(10)	0.0002(9)

Table S2c. Pertinent interatomic distances (\AA) and corresponding bond-valence sum calculations for $\text{Ba}_2\text{Fe}(\text{As}_3\text{O}_6)_2\cdot\text{H}_2\text{O}$.

Ba		Fe		As	
Ba_1—O1_1	2.776(8)	Fe—O1_1	2.174(9)	As2_2—O2_2	1.829(10)
Ba_1—O1_1	2.968(9)	Fe—O1_2	2.174(9)	As2_2—O5_2	1.819(12)
Ba_1—O2_1	2.992(9)	Fe—O4_1	2.192(10)	As2_2—O6_2	1.712(10)
Ba_1—O2_1	2.812(10)	Fe—O4_2	2.192(10)	-	-
Ba_1—O4_1	2.689(10)	Fe—O6_1	2.072(10)	As3_1—O1_1	1.708(9)
Ba_1—O4_1	2.974(10)	Fe—O6_2	2.072(10)	As3_1—O2_1	1.861(10)
Ba_1—O5_2	2.956(12)	As		As3_1—O3_1	1.817(9)
Ba_1—O6_2	2.739(10)	As1_1—O3_1	1.823(9)	-	-
Ba_1—O7_1	3.033(7)	As1_1—O4_1	1.702(10)	As3_2—O1_2	1.711(9)
-	-	As1_1—O5_1	1.753(12)	As3_2—O2_2	1.857(10)
Ba_2—O1_2	2.776(8)	-	-	As3_2—O3_2	1.822(9)
Ba_2—O1_2	2.968(9)	As1_2—O3_2	1.823(9)	H	
Ba_2—O2_2	2.992(9)	As1_2—O4_2	1.702(10)	H_1—O7_1	0.901(8)
Ba_2—O2_2	2.812(10)	As1_2—O5_2	1.753(12)	H_1—H_2	1.471(1)
Ba_2—O4_2	2.689(10)	-	-	-	-
Ba_2—O4_2	2.974(10)	As2_1—O2_1	1.829(10)	H_2—O7_1	0.900(11)
Ba_2—O5_1	2.956(12)	As2_1—O5_1	1.819(12)	H_2—H_1	1.471(1)
Ba_2—O6_1	2.739(10)	As2_2—O6_1	1.712(10)	-	-
Ba_2—O6_2	3.160(10)	-	-	-	-
BVS Ba_1	2.02(2)	BVS Ba_2	1.89(2)	BVS Fe	1.99(2)
BVS As1_1	3.21(4)	BVS As1_2	3.18(4)	BVS As2_1	2.97(4)
BVS As2_2	3.00(4)	BVS As3_1	2.97(4)	BVS As3_2	2.93(4)
BVS O1_1	1.93(3)	BVS O1_2	1.92(3)	BVS O2_1	2.20(3)
BVS O2_2	2.11(3)	BVS O3_1	1.96(3)	BVS O3_2	2.12(3)
BVS O4_1	1.97(3)	BVS O4_2	1.97(3)	BVS O5_1	2.21(4)
BVS O5_2	2.26(4)	BVS O6_1	1.98(3)	BVS O6_2	1.98(3)
BVS O7_1	1.61(1)	BVS H_1	1.02(1)	BVS H_2	1.04(1)

Table S2d. Atomic positions and equivalent isotropic thermal displacement (in Å²) for BaFe₂As₂O₅AsO₃OH.

Atom	Wick.	Site	x	y	z	Ueq (Å²)
Ba (2+)	4g	..m	0.3206(1)	0.2510(2)	0	0.0200(6)
Fe (3+)	8i	1	0.2569(2)	0.0017(4)	0.3279(2)	0.0193(9)
As1 (3+)	8i	1	0.4248(2)	0.7419(2)	-0.1860(2)	0.0198(7)
As2 (3+)	4h	..m	0.1099(3)	-0.1952(3)	1/2	0.0229(11)
O1 (2-)	8i	1	0.3351(10)	0.5741(15)	-0.1680(14)	0.024(3)
O2 (2-)	8i	1	0.3464(10)	-0.0698(15)	0.1706(13)	0.019(3)
O3 (2-)	8i	1	0.3115(8)	0.2510(14)	0.3471(11)	0.014(2)
O4 (2-)	4g	..m	0.5239(13)	0.263(2)	0	0.022(4)
O5 (2-)	4h	..m	0.1563(12)	0.0333(19)	1/2	0.011(4)
O6 (2-)	4h	..m	0.3481(18)	-0.060(3)	1/2	0.038(6)
H (1+)	4h	..m	0.406(16)	-0.13(4)	1/2	0.12(14)

Table S2e. Anisotropic thermal displacement (in Å²) for BaFe₂As₂O₅AsO₃OH.

Atom	U₁₁	U₂₂	U₃₃	U₁₂	U₁₃	U₂₃
Ba	0.0251(12)	0.0204(8)	0.0144(9)	-0.0005(10)	0.0000	0.0000
Fe	0.029(2)	0.0187(12)	0.0106(13)	0.0000(14)	-0.0009(18)	-0.0011(12)
As1	0.0250(14)	0.0226(10)	0.0118(10)	-0.0006(11)	0.0027(9)	0.0001(8)
As2	0.032(2)	0.0263(16)	0.0103(16)	0.0010(15)	0.0000	0.0000

Table S2f. Pertinent interatomic distances (\AA) and corresponding bond-valence sum calculations for $\text{BaFe}_2\text{As}_2\text{O}_5\text{AsO}_3\text{OH}$.

Ba		Fe		As	
Ba—O1	2.830(12)	Fe—O1	1.982(13)	As1—O1	1.745(13)
Ba—O1	2.912(13)	Fe—O2	1.942(13)	As1—O2	1.757(12)
Ba—O1	2.830(12)	Fe—O3	1.990(11)	As1—O4	1.816(7)
Ba—O1	2.912(13)	Fe—O3	2.077(11)	-	-
Ba—O2	2.843(11)	Fe—O5	2.082(11)	-	-
Ba—O2	3.045(12)	Fe—O6	2.037(15)	As2—O3	1.789(11)
Ba—O2	2.843(11)	Fe—Fe	3.102(3)	As2—O3	1.789(11)
Ba—O2	3.045(12)	Fe—As2	2.919(4)	As2—O5	1.800(15)
Ba—O3	3.131(10)	-	-	As2—O6	2.759(15)
Ba—O3	3.131(10)	-	-	H	
Ba—O4	2.768(18)	-	-	H—O6	1.0(3)
BVS Ba	2.00(2)	BVS Fe	3.06(4)	-	-
BVS As1	3.15(5)	BVS As2	3.04(6)	BVS H	0.92(5)
BVS O1	2.10(4)	BVS O2	2.07(4)	BVS O3	2.08(4)
BVS O4	2.13(3)	BVS O5	1.84(4)	BVS O6	1.9(5)

Table S2g. Atomic positions and equivalent isotropic thermal displacement (in \AA^2) for $\text{Ba}_2\text{Fe}_2\text{O}(\text{As}_2\text{O}_5)_2$.

Atom	Wick.	Site	x	y	z	Ueq (\AA^2)
Ba (2+)	8h	m.2m	0.6722(1)	0.1722(1)	0	0.0091(1)
Fe (3+)	8f	4..	1/2	1/2	0.8604(1)	0.0072(1)
As (3+)	16l	..m	0.8639(1)	0.3639(1)	0.8345(1)	0.0086(1)
O1 (2-)	8g	2.mm	1/2	0	0.1175(2)	0.0123(5)
O2 (2-)	32m	1	0.7093(1)	0.4241(1)	0.8965(1)	0.0120(3)
O3 (2-)	4a	422	1/2	1/2	3/4	0.0210(8)

Table S2h. Anisotropic thermal displacement (in \AA^2) for $\text{Ba}_2\text{Fe}_2\text{O}(\text{As}_2\text{O}_5)_2$.

Atom	U ₁₁	U ₂₂	U ₃₃	U ₁₂	U ₁₃	U ₂₃
Ba	0.0085(1)	0.0085(1)	0.0103(1)	-0.0006(1)	0.0000	0.0000
Fe	0.0065(1)	0.0065(1)	0.0086(2)	0.0000	0.0000	0.0000
As	0.0082(1)	0.0082(1)	0.0094(1)	-0.0009(1)	-0.0003(1)	-0.0003(1)
O1	0.0105(6)	0.0105(6)	0.0158(12)	0.0039(9)	0.0000	0.0000
O2	0.0074(5)	0.0120(6)	0.0165(6)	0.0013(4)	0.0005(4)	0.0012(5)
O3	0.0253(12)	0.0253(12)	0.0124(17)	0.0000	0.0000	0.0000

Table S2i. Pertinent interatomic distances (\AA) and corresponding bond-valence sum calculations for $\text{Ba}_2\text{Fe}_2\text{O}(\text{As}_2\text{O}_5)_2$.

Ba		Fe	
Ba—O1	2.8342(17)	Fe—O2 2.0152(11)	
Ba—O1	2.8342(17)	Fe—O2 2.0152(11)	
Ba—O2	2.7660(13)	Fe—O2 2.0152(11)	
Ba—O2	2.9085(13)	Fe—O2 2.0152(11)	
Ba—O2	2.9086(13)	Fe—O3 1.7775(6)	
Ba—O2	2.7660(13)	Fe—Fe 3.5551(8)	
Ba—O2	2.7660(13)	As	
Ba—O2	2.9085(13)	As—O1 1.8391(11)	
Ba—O2	2.9086(13)	As—O2 1.7503(12)	
Ba—O2	2.7660(13)	As—O2 1.7503(12)	
BVS Ba	2.285(3)	BVS Fe 2.2953(4)	
BVS As	3.094(6)	BVS O1 2.200(4)	
BVS O2	2.069(4)	BVS O3 1.902(2)	

Table S2j. Atomic positions and equivalent isotropic thermal displacement (in \AA^2) for $\text{Fe}_3(\text{As}_2\text{O}_5)(\text{AsO}_3)\text{Cl}$.

Atom	Wick.	Site	x	y	z	Ueq (\AA^2)
Fe1 (3+)	1a	-1	0	0	0	0.0084(5)
Fe2 (2+)	1h	-1	1/2	-1/2	1/2	0.0137(6)
Fe3 (3+)	2i	1	0.58463(19)	-0.27586(12)	0.12719(11)	0.0081(4)
Fe4 (2.5+)	2i	1	-0.3011(2)	0.34295(13)	0.12287(12)	0.0101(4)
As1 (3+)	2i	1	0.28644(14)	0.07443(9)	0.21285(8)	0.0092(3)
As2 (3+)	2i	1	0.89118(14)	-0.23947(9)	0.34916(8)	0.0100(3)
As3 (3+)	2i	1	0.15656(15)	-0.54602(10)	0.23166(9)	0.0138(3)
Cl1 (1-)	2i	1	-0.3176(4)	0.2558(2)	0.3881(2)	0.0188(7)
O1 (2-)	2i	1	0.8363(9)	-0.1512(6)	0.1583(5)	0.0094(11)
O2 (2-)	2i	1	0.3685(9)	-0.4411(6)	0.1084(5)	0.0116(11)
O3 (2-)	2i	1	0.6417(9)	-0.3396(6)	0.3477(5)	0.0115(11)
O4 (2-)	2i	1	0.3104(9)	-0.0864(6)	0.1246(5)	0.0101(11)
O5 (2-)	2i	1	0.4505(9)	0.2098(6)	0.0899(5)	0.0079(10)
O6 (2-)	2i	1	-0.1295(9)	0.5302(6)	0.1290(5)	0.0110(11)
O7 (2-)	2i	1	-0.0125(9)	0.1621(6)	0.1198(5)	0.0103(11)
O8 (2-)	2i	1	1.1425(9)	-0.4177(6)	0.3521(5)	0.0117(11)

Table S2k. Anisotropic thermal displacement (in Å²) for Fe₃(As₂O₅)(AsO₃)Cl.

Atom	U ₁₁	U ₂₂	U ₃₃	U ₁₂	U ₁₃	U ₂₃
Fe1	0.0052(8)	0.0088(7)	0.0103(8)	-0.0029(6)	0.0007(7)	-0.0007(6)
Fe2	0.0112(9)	0.0178(8)	0.0112(8)	-0.0094(7)	0.0026(7)	0.0011(6)
Fe3	0.0044(5)	0.0089(5)	0.0111(6)	-0.0012(4)	0.0004(5)	-0.0031(4)
Fe4	0.0054(6)	0.0119(5)	0.0135(6)	-0.0026(4)	0.0016(5)	-0.0041(4)
As1	0.0064(4)	0.0110(4)	0.0106(4)	-0.0039(3)	0.0013(3)	-0.0024(3)
As2	0.0052(4)	0.0142(4)	0.0112(4)	-0.0035(3)	-0.0006(3)	-0.0037(3)
As3	0.0068(4)	0.0152(4)	0.0186(5)	-0.0037(3)	0.0007(4)	-0.0030(3)
Cl1	0.0145(10)	0.0223(10)	0.0164(10)	-0.0026(8)	0.0005(9)	-0.0022(8)

Table S2l. Pertinent interatomic distances (Å) and corresponding bond-valence sum calculations for Fe₃(As₂O₅)(AsO₃)Cl.

As	Fe	Fe
As1—Fe1 2.8910(12)	Fe1—O1 2.019(5)	Fe3—Fe4 3.196(2)
As1—O4 1.802(6)	Fe1—O1 2.019(5)	Fe3—Fe4 3.136(2)
As1—O5 1.774(5)	Fe1—O4 1.978(5)	Fe3—O1 1.991(6)
As1—O7 1.791(5)	Fe1—O4 1.978(5)	Fe3—O2 2.073(6)
- -	Fe1—O7 2.042(6)	Fe3—O3 2.035(5)
As2—Fe3 2.8649(17)	Fe1—O7 2.042(6)	Fe3—O4 1.972(5)
As2—O1 1.764(5)	- -	Fe3—O5 1.992(5)
As2—O3 1.768(6)	Fe2—Cl1 2.645(2)	Fe3—O6 2.038(5)
As2—O8 1.832(5)	Fe2—Cl1 2.645(2)	- -
- -	Fe2—O3 1.961(5)	Fe4—Cl1 2.441(3)
As3—Fe4 3.1668(18)	Fe2—O3 1.961(5)	Fe4—O2 2.286(5)
As3—Cl1 3.179(2)	Fe2—O8 2.303(5)	Fe4—O2 2.134(5)
As3—O2 1.831(5)	Fe2—O8 2.303(5)	Fe4—O5 2.035(6)
As3—O5 3.024(5)	- -	Fe4—O6 2.033(6)
As3—O6 1.766(5)	- -	Fe4—O7 1.988(5)
As3—O8 1.811(6)	- -	- -
BVS As1 3.00(2)	BVS As2 3.02(2)	BVS As3 2.94(2)
BVS Fe1 3.030(17)	BVS Fe2 2.064(12)	BVS Fe3 3.001(17)
BVS Fe4 2.480(14)	- -	BVS Cl1 0.611(3)
BVS O1 2.099(17)	BVS O2 1.925(15)	BVS O3 2.112(19)
BVS O4 2.081(18)	BVS O5 2.084(17)	BVS O6 2.012(17)
BVS O7 1.998(16)	BVS O8 2.063(19)	- -

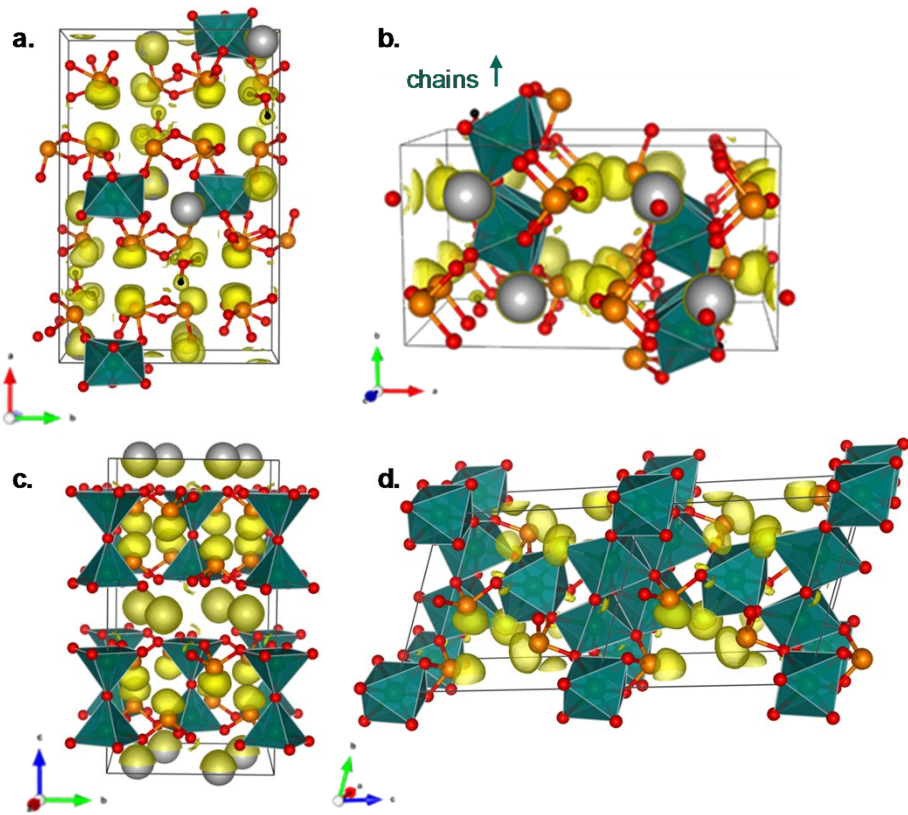


Figure S2m. Snapshots of the ELF function with evidence of the As^{3+} electronic lone pair (in yellow) from DFT calculations for $\text{Ba}_2\text{Fe}(\text{As}_3\text{O}_6)_2\cdot\text{H}_2\text{O}$, $\text{BaFe}_2\text{As}_2\text{O}_5\text{AsO}_3\text{OH}$, $\text{Ba}_2\text{Fe}_2\text{O}(\text{As}_2\text{O}_5)_2$ and $\text{Fe}_3(\text{As}_2\text{O}_5)(\text{AsO}_3)\text{Cl}$ (a,b,c,d respectively). These representations were drawn at $\eta(r) = 0.7379, 0.7232, 0.7155$ and 0.7010 isosurface respectively.

INFRARED SPECTROSCOPIES

For $\text{BaFe}_2\text{As}_2\text{O}_5\text{AsO}_3\text{OH}$ (compound **(2)**), the structure being rather complex mixing ortho and pyro-arsenites, the precise assignment of all the bands is complicated, by band overlap, and possible contribution of secondary phases. However, the presence of hydroxides is confirmed by a stretching and in plane deformation modes seen around 3435 and 1415 cm^{-1} respectively (see Fig. 2a, marked in blue). As-O stretching modes in As_2O_5 groups and AsO_3 groups respectively can be seen around 895 and 875/840 cm^{-1} region, while the bands around 675/615 cm^{-1} correspond to stretching modes in $\text{AsO}_2\text{-O-AsO}_2$ bridges groups.¹⁻⁴ Bands around 520, 440 and 415 cm^{-1} might be assigned to various As-O bending modes. Finally, the bands around 855, 777, 700 cm^{-1} are assigned to Fe-O bending in iron octahedra.

In the case of $\text{Fe}_3(\text{As}_2\text{O}_5)(\text{AsO}_3)\text{Cl}$ (compound **(4)**) most of the bands related to chloride bonding are usually found below 400 cm^{-1} , thus not shown here.⁴ Similarly to compound **(1)**, the bands observed around 750, 665 and 610 cm^{-1} can be attributed to As-O stretching in AsO_3 , As_2O_5 and $\text{AsO}_2\text{-O-AsO}_2$ groups respectively, while the bands around 525, 480 and 430 cm^{-1} can be attributed to bending modes in As_2O_5 , AsO_3 and $\text{AsO}_2\text{-O-AsO}_2$ groups.¹⁻⁴ However, one must note that the Fe-O stretching vibration in iron octahedra can also be seen in the 750 and 650 cm^{-1} domain, making it difficult to exactly assign the bands.⁴

1 F. A. Miller and C. H. Wilkins, *Infrared Spectra and Characteristic Frequencies of Inorganic Ions*, Anal. Chem., 1952, **24**, 1253–1294.

2 H. A. Szymanski, L. Marabella, J. Hoke and J. Harter, *Infrared and Raman Studies of Arsenic Compounds*, Appl. Spectrosc., 1968, **22**, 297–304.

3 S. Goldberg and C. T. Johnston, *Mechanisms of arsenic adsorption on amorphous oxides evaluated using macroscopic measurements, vibrational spectroscopy, and surface complexation modeling*, J. Colloid Interface Sci., 2001, **234**, 204–216.

4 K. Nakamoto, *Infrared and Raman Spectra of Inorganic and Coordination Compounds: Part A: Theory and Applications in Inorganic Chemistry*, 2009.

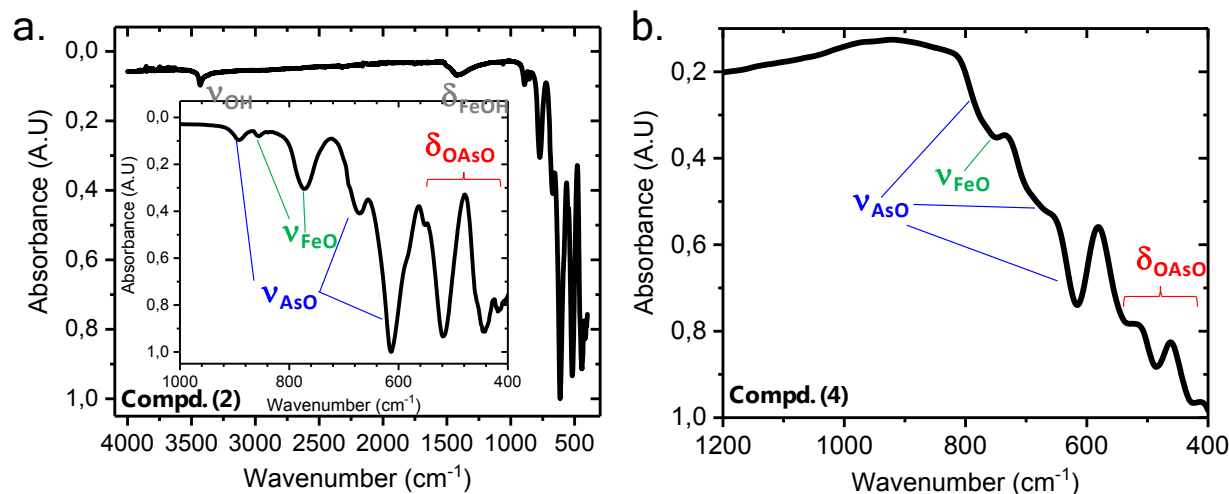


Figure S2n. Spectroscopies: a) IR spectra for $\text{BaFe}_2(\text{As}_2\text{O}_5)(\text{AsO}_3)(\text{OH})$ (compound **(2)**). b) IR spectra for $\text{Fe}_3(\text{As}_2\text{O}_5)(\text{AsO}_3)\text{Cl}$ (compound **(4)**).

(S3) EDS-SEM analysis.

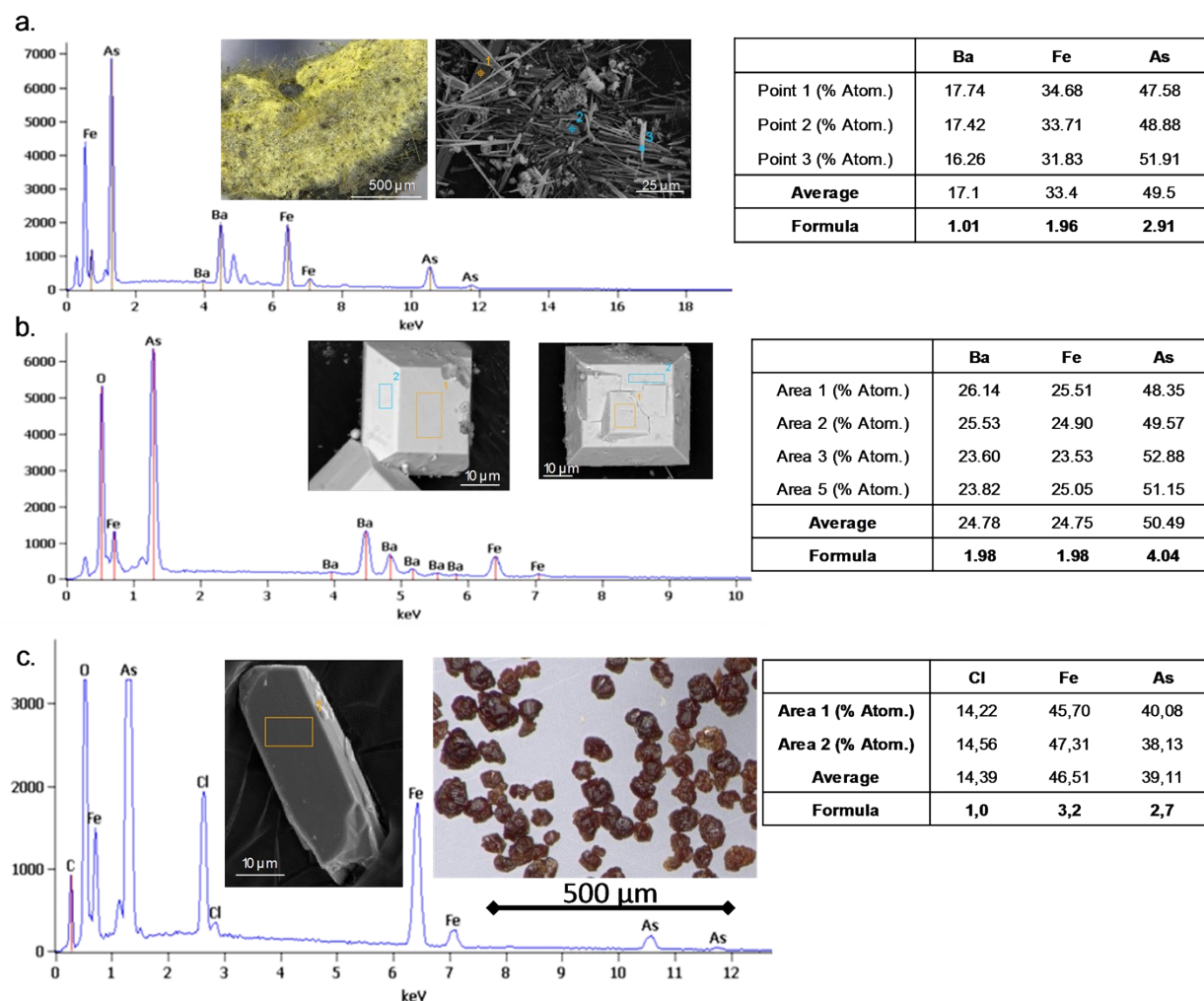


Figure S3. EDS-SEM analysis, and resulting formula obtained from several averaged % Atomic points acquisition for $\text{BaFe}_2\text{As}_2\text{O}_5\text{AsO}_3\text{OH}$, $\text{Ba}_2\text{Fe}_2\text{O}(\text{As}_2\text{O}_5)_2$ and $\text{Fe}_3(\text{As}_2\text{O}_5)(\text{AsO}_3)\text{Cl}$ (a,b,c respectively).

(S4) DFT calculations details.

Table S4a. Relative energies for the different magnetic configurations used to extract the two magnetic exchanges parameters (J_1 , J_2) within $\text{Ba}_2\text{Fe}(\text{As}_3\text{O}_6)_2\text{-H}_2\text{O}$ structure, at $U_{\text{eff}} = 6 \text{ eV}$. The most stable configuration was shifted to $E = 0$. The values are really low, in agreement with our statement (highly disconnected octahedral leading to a paramagnetic behaviour). FM values are represented negative, while AFM are positive.

$\text{Ba}_2\text{Fe}(\text{As}_3\text{O}_6)_2\text{-H}_2\text{O}$		$U = 6 \text{ eV}$
Relative energies (eV/unit cell)	FM	0.00155
	AF1	0.00028
	AF2	0.00199
	AF3	0
Spin exchange parameters (K)	J1	+0.23
	J2	-0.14

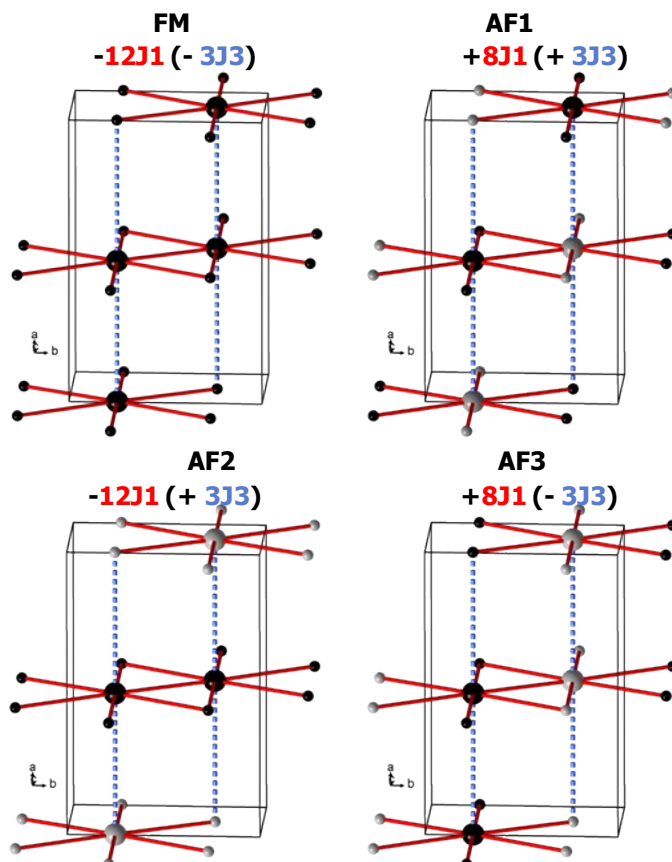


Figure S4b. Representation of the four ordered spin states (FM, AF1, AF2, AF3) employed to probe the magnetically disconnected and paramagnetic behaviour of $\text{Ba}_2\text{Fe}(\text{As}_3\text{O}_6)_2\text{-H}_2\text{O}$ structure. Only Fe^{3+} sites are represented for clarity. Up spin Fe^{3+} sites are represented in black filled circles, while down spins are represented in white filled circle. The 4 Fe^{3+} cations inside the primitive cell display larger radius.

Table S4c. Values of the geometrical parameters (distances in Å and angles in °) along the magnetic exchanges paths for BaFe₂As₂O₅AsO₃OH structure a x b x 2c cell at U = 6 eV. FM values are represented negative, while AFM are positive.

Path	Path	Fe...Fe (Å)	Fe-O (Å)	O...O (Å)	O-Fe (Å)	∠ Fe-O-Fe ↑ Fe-O-O-Fe (deg)	U = 6 eV J (K)
SE							
J1	In chains	3.104(1)	2.035(1)	-	2.035(1)	99	+28.56
J2	In chains	3.691(1)	2.077(1)	-	1.988(1)	130.5	+6.57
SSE							
Jd	In chains	4.823(1)	1.988(1)	2.542(1)	2.084(1)	187.5	-3.29
« No path »							
J3	Between Chains	5.910(2)	-	-	-	« 0 »	+0.69
J4	Between Layers	6.619(3)	-	-	-	« 79.2 »	-0.003

Table S4d. Relative energies for the different magnetic configurations used to extract the magnetic exchanges parameters for BaFe₂As₂O₅AsO₃OH structure within a a x b x 2c, and U_{eff} = 6 eV. The most stable configuration was shifted to E = 0. FM values are represented negative, while AFM are positive.

BaFe ₂ (As ₂ O ₅)(AsO ₃)(OH)		U = 6 eV
Relative energies (eV/unit cell)	FM	0.59926
	AF1	0.44403
	AF2	0.00594
	AF3	0
	AF4	0.59287
	AF5	0.58782
	AF6	0.0474
	AF7	0.43862
	AF8	0.00005
	AF9	0.59926
Spin exchange parameters (K) (- = FM + = AFM)	J1 J2 Jd Jinter J4	+28.56 +6.57 -3.29 +0.69 -0.003
	Total θc (K)	-55.03

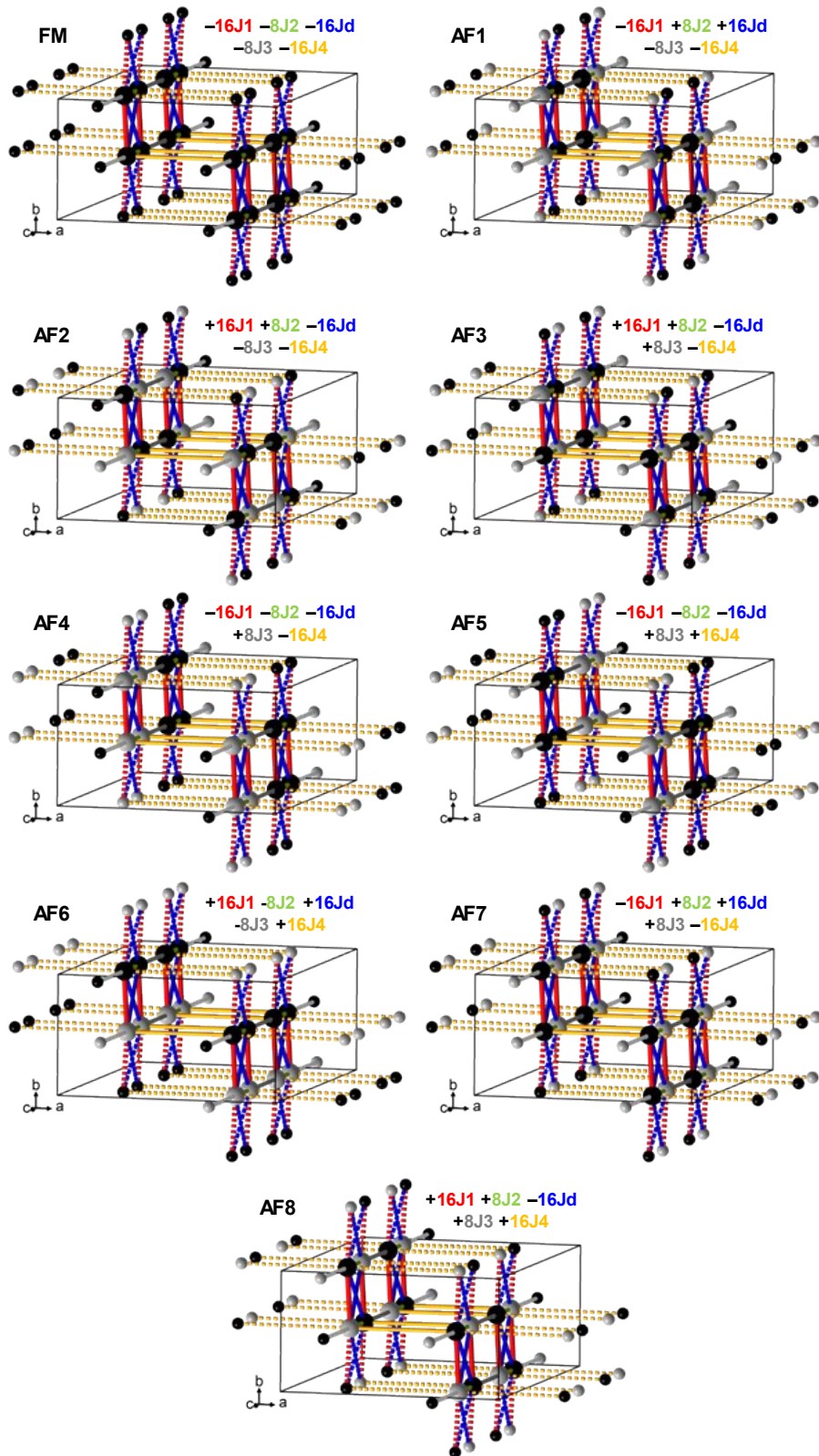


Figure S4e. Representation of the nine ordered spin states (FM, AF1, AF2, AF3, AF4, AF5, AF6, AF7, AF8) employed to extract the five spin exchanges parameters (J_1, J_2, J_d, J_3, J_4) for $\text{BaFe}_2\text{As}_2\text{O}_5\text{AsO}_3\text{OH}$ structure within a “ $a \times b \times 2c$ ”. Only Fe^{3+} sites are represented for clarity. Up spin Fe^{3+} sites are represented in black filled circles, while down spin are represented in white filled circle. The 16 Fe^{3+} cations inside the primitive cell display larger radius.

Table S4f. Values of the geometrical parameters (distances in Å and angles in °) along the magnetic exchanges paths for $\text{Ba}_2\text{Fe}_2\text{O}(\text{As}_2\text{O}_5)_2$ structure at $U = 7 \text{ eV}$. FM values are represented negative, while AFM are positive.

Path	Path	Fe...Fe (Å)	Fe-O (Å)	O...O (Å)	O-Fe (Å)	\angle Fe-O-Fe τ Fe-O-O-Fe (deg)	U = 7 eV J (K)
SE							
Jdim	In dimers	3,555(1)	1,778(1)	-	1,778(1)	180	+259.03
SSE							
J2	Between dimers	6,128(1)	2,015(1)	2,633(2)	2,015(1)	180	-3.33
No path							
J3	Between Layers	4.498(1)	-	-	-	« 180 »	+1.28

Table S4g. Relative energies for the different magnetic configurations used to extract the magnetic exchanges parameters for $\text{Ba}_2\text{Fe}_2\text{O}(\text{As}_2\text{O}_5)_2$ structure, and $U_{\text{eff}} = 4 \text{ eV}$ to 7 eV . The most stable configurations were shifted to $E = 0$ for each U_{eff} values. FM values are represented negative, while AFM are positive.

$\text{Ba}_2\text{Fe}_2\text{O}(\text{As}_2\text{O}_5)_2$		$U = 4 \text{ eV}$	$U = 6 \text{ eV}$	$U = 7 \text{ eV}$
Relative energies (eV/unit cell)	FM	1.76997	1.35769	1.17905
	AF1	1.76057	1.35112	1.17353
	AF2	0.09374	0.06626	0.05523
	AF3	1.66171	1.28189	1.11606
	AF4	0	0	0
Spin exchange parameters (K) (- = FM + = AFM)	Jdim	+385.666	+297.514	+259.027
	J2	-5.736	-4.017	-3.335
	J3	+2.182	+1.525	+1.281
	Total θc (K)	-373.508	-288.997	-251.971

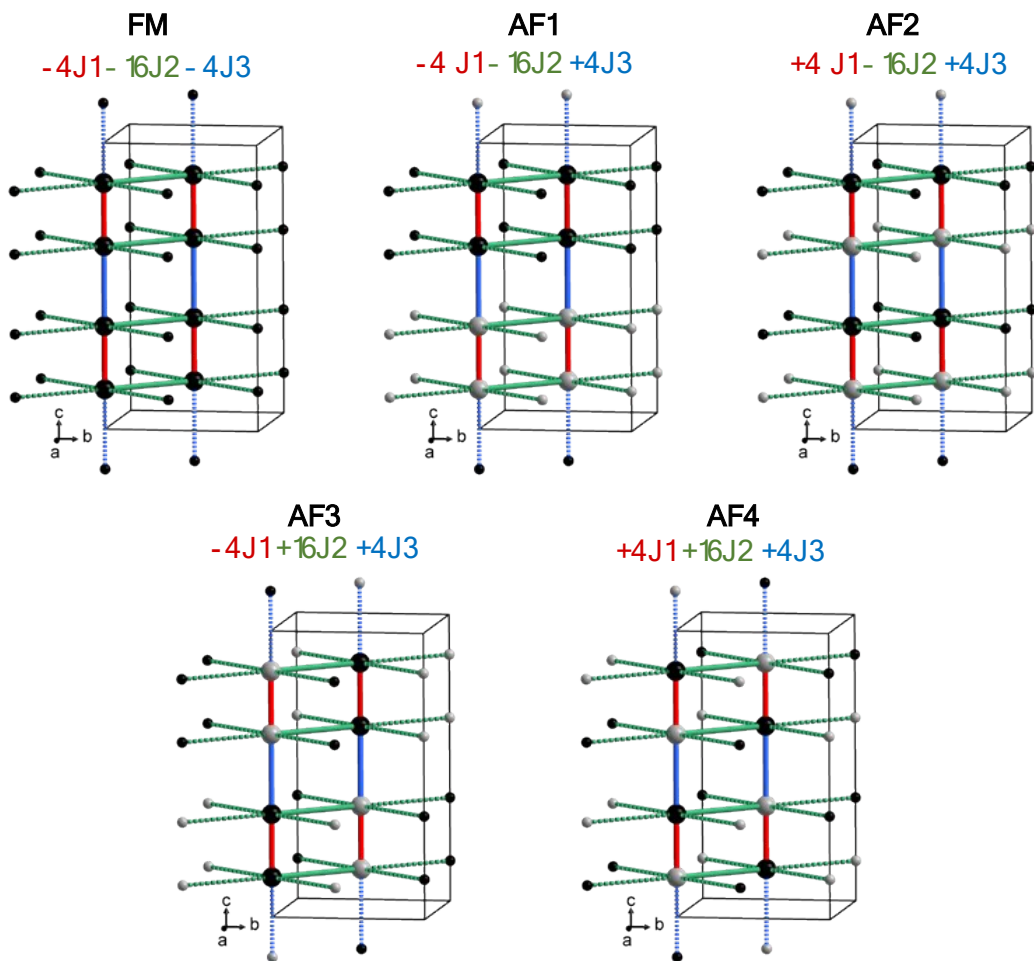


Figure S4h. Representation of the five ordered spin states (FM, AF1, AF2, AF3, AF4) employed to extract the three spin exchange parameters (J_1 , J_2 , J_3) for $\text{Ba}_2\text{Fe}_2\text{O}(\text{As}_2\text{O}_5)_2$ structure. Only Fe^{3+} sites are represented for clarity. Up spin Fe^{3+} sites are represented in black filled circles, while down spin are represented in white filled circle. The 8 Fe^{3+} cations inside the primitive cell display larger radius.

Table S4i. Values of the geometrical parameters (distances in Å and angles in °) along the magnetic exchanges paths for $\text{Fe}_3(\text{As}_2\text{O}_5)(\text{AsO}_3)\text{Cl}$ structure at $U = 6$ eV. FM values are represented negative, while AFM are positive.

Path	Path	Fe...Fe (Å)	Fe-O (Å)	O...O (Å)	O-Fe (Å)	$\angle \text{Fe}-\text{O}-\text{Fe}$ $\tau \text{Fe}-\text{O}-\text{O}-\text{Fe}$ (deg)
SE						
J1	Fe4-Fe4	3.384(1)	2.286(5)	-	2.1334(5)	99.9(2)
J2	Fe3-Fe2	3.5981(1)	1.961(5)	-	2.035 (5)	128.4(3)
J3 (Cl)	Fe4-Fe2	4.297(1)	2.441(2)	-	2.646(2)	115.26(8)
J4	Fe3-Fe4	3.196(2)	2.286(5)	-	2.073(6)	94.1(2)
J5	Fe4-Fe1	3.578(1)	1.988(5)	-	2.042(6)	125.2(3)
J6	Fe3-Fe4	3.136(2)	2.073(6)	-	2.134(5)	94.4(2)
J6	-	-	1.993(5)	-	2.035(6)	102.2(2)
J7	Fe3-Fe1	3.5645(9)	1.972 (5)	-	1.977(5)	128.9(3)
J8	Fe3-Fe1	3.571(1)	1.991(6)	-	2.019(5)	125.9(3)
SSE						
J9	Fe3-Fe3	5.353(2)	2.073(6)	2.848(7)	2.073(6)	180.0(2)
J10	Fe4-Fe1	5.630(1)	2.042(6)	2.676(7)	2.035(6)	171.0(4)
J11	Fe1-Fe1	5.5346(1)	1.977(5)	2.851(7)	2.019(5)	25.7(6)

Table S4j. Relative energies for the different magnetic configurations used to extract the magnetic exchanges parameters trends for $\text{Fe}_3(\text{As}_2\text{O}_5)(\text{AsO}_3)\text{Cl}$ structure at $U = 6$ eV. The most stable configurations were shifted to $E = 0$ for each U_{eff} values.

Fe3(As2O5)(AsO3)Cl		U = 6 eV
Relative energies (eV/unit cell)	FM	0.03715
	AF1	0.00494
	AF2	0.00297
	AF3	0
	AF4	0.00121
	AF5	0.14171

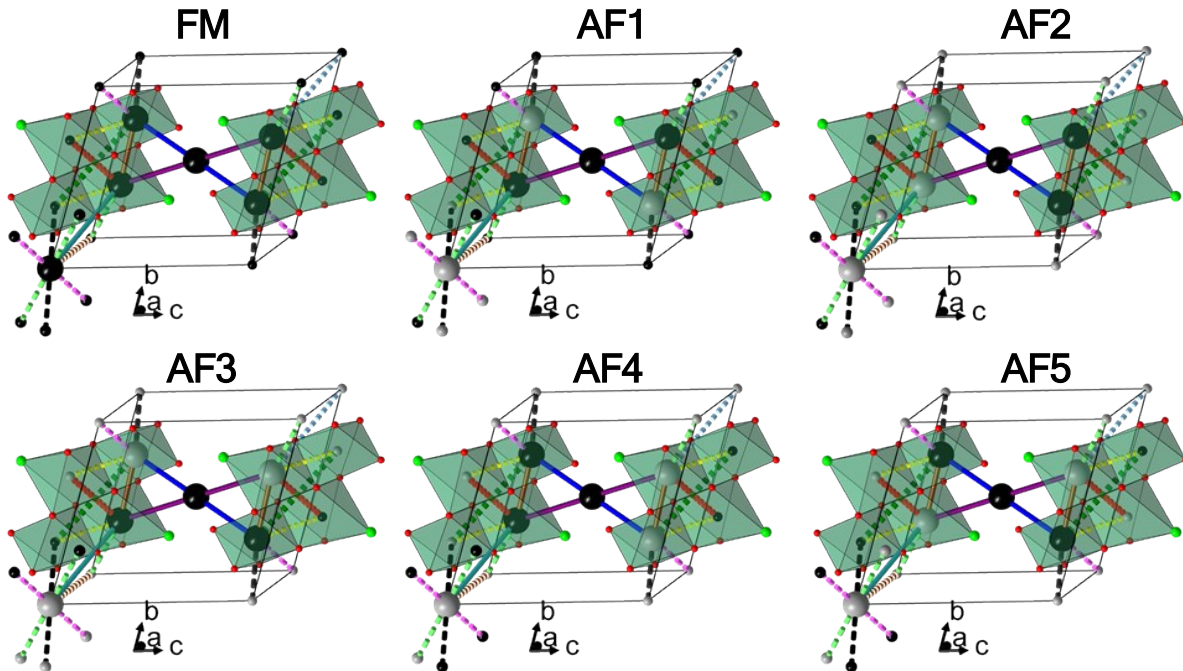


Figure S4k. Representation of the six pertinent ordered spin states (FM, AF1, AF2, AF3, AF4, AF5) employed to extract the global trends in couplings for $\text{Fe}_3(\text{As}_2\text{O}_5)(\text{AsO}_3)\text{Cl}$ structure, within a single unit cell. Only Fe^{3+} sites are represented for clarity. Up spin Fe^{3+} sites are represented in black filled circles, while down spin are represented in white filled circle. The 6 Fe cations inside the primitive cell display larger radius.

Table S4l. Comparison between the crystallographically calculated BVS and obtained magnetic moment (in μ_B/Fe) from DFT calculations for each Fe cations within the simple cell $\text{Fe}_3(\text{As}_2\text{O}_5)(\text{AsO}_3)\text{Cl}$ structure at $U = 6 \text{ eV}$. The results are in favour of a $\text{Fe}^{3+}/\text{Fe}^{2+}$ charge ordering on the Fe4 sites.

	BVS	FM ($U = 6 \text{ eV}$)	AF1 ($U = 6 \text{ eV}$)	AF2 ($U = 6 \text{ eV}$)	AF3 ($U = 6 \text{ eV}$)	AF4 ($U = 6 \text{ eV}$)	AF5 ($U = 6 \text{ eV}$)
	M (μ_B/Fe)	M (μ_B/Fe)	M (μ_B/Fe)	M (μ_B/Fe)	M (μ_B/Fe)	M (μ_B/Fe)	M (μ_B/Fe)
Fe1	3.03(2)	4.376	4.355	4.345	4.346	4.345	4.333
Fe2	2.06(1)	3.769	3.741	3.750	3.749	3.749	3.762
Fe3	3.00(2)	4.357	4.340	4.348	3.444	4.330	4.330
Fe4	2.48(2)	4.335	3.730	4.323	3.733	3.731	4.063
		3.767	4.308	3.731	4.321	4.323	4.096

(S5) Magnetic measurements details.

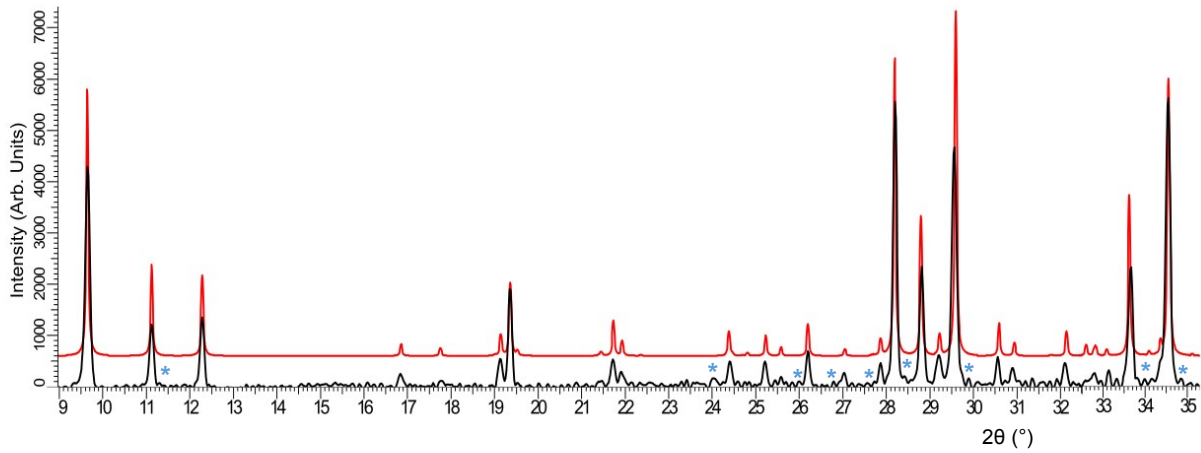


Figure S5a. Comparison between the experimental measured XRD powder diagram (in black) and the simulated one from our crystallographic model (in red) for $\text{Fe}_3(\text{As}_2\text{O}_5)(\text{AsO}_3)\text{Cl}$. Blue stars stand for the impurity peaks, identified as $\gamma\text{-Fe}_2\text{O}_3$.

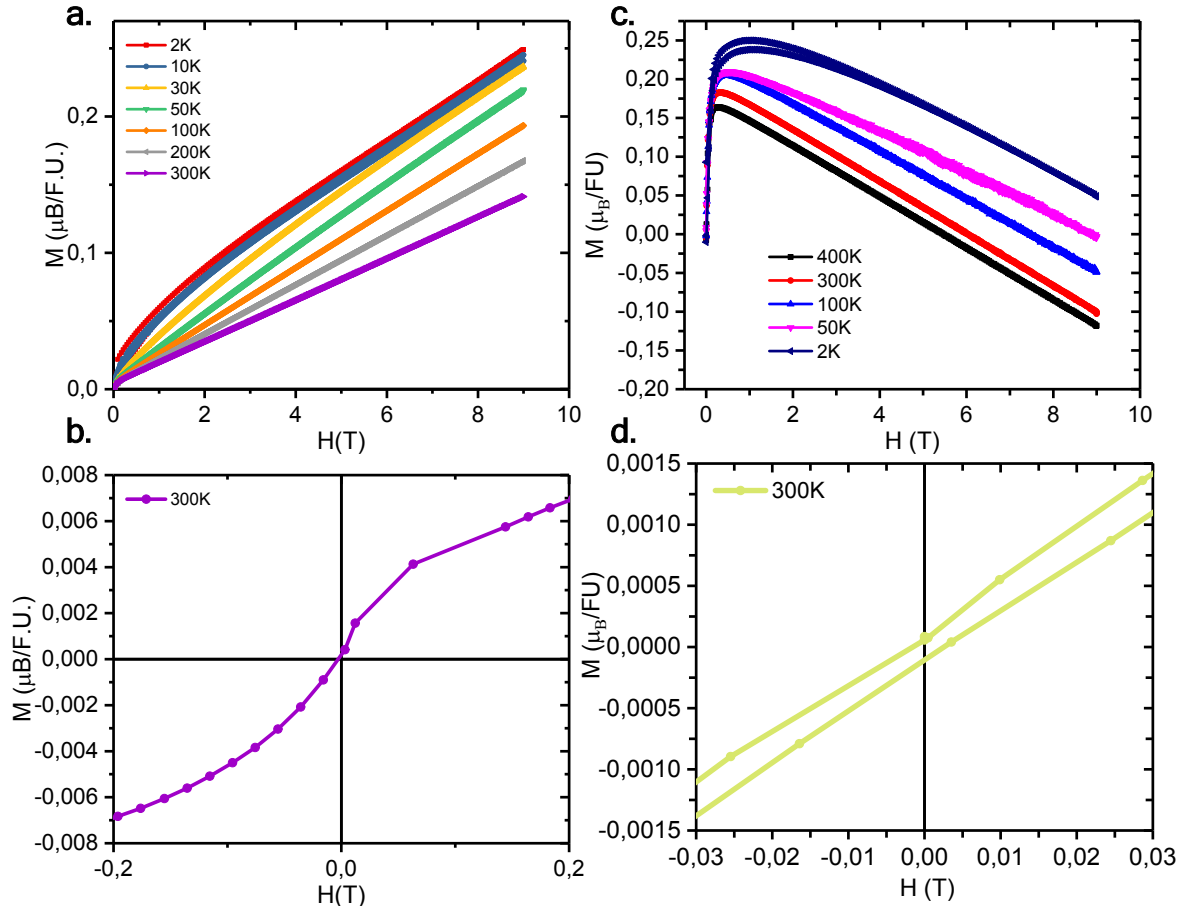


Figure S5b. a) $M(H)$ measurement between 0 and 9 T for $\text{BaFe}_2(\text{As}_2\text{O}_5)(\text{AsO}_3)(\text{OH})$, b) Highlighting the hysteresis at room temperature due to the presence of magnetic impurity in the sample. c) $M(H)$ measurement between 0 and 9 T for $\text{Ba}_2\text{Fe}_2\text{O}(\text{As}_2\text{O}_5)_2$ d) Highlighting the small hysteresis observed in the $\text{Fe}_3(\text{As}_2\text{O}_5)(\text{AsO}_3)\text{Cl}$ magnetic measurements, resulting from the presence of $\gamma\text{-Fe}_2\text{O}_3$.